Mon. Not. R. Astron. Soc. **000**, 1–9 (2010) Printed 20 October 2010 (MN LaTeX style file v2.2)

On the Effects of Coupled Scalar Fields on Structure Formation

Baojiu Li[1,2,⋆], John D. Barrow[1,†]
[1] *DAMTP, Centre for Mathematical Sciences, University of Cambridge, Wilberforce Road, Cambridge CB3 0WA, UK*
[2] *Kavli Institute for Cosmology Cambridge, Madingley Road, Cambridge CB3 0HA, UK*

20 October 2010

ABSTRACT
A coupling between a scalar field (representing the dark energy) and dark matter could produce rich phenomena in cosmology. It affects cosmic structure formation mainly through the fifth force, a velocity-dependent force that acts parallel to particle's direction of motion and proportional to its speed, an effective rescaling of the particle masses, and a modified background expansion rate. In many cases these effects entangle and it is difficult to see which is the dominant one. Here we perform N-body simulations to study their qualitative behaviour and relative importance in affecting the key structure formation observables, for a model with exponential scalar field coupling. We find that the fifth force, a prominent example of the scalar-coupling effects, is far less important than the rescaling of particle mass or the modified expansion rate. In particular, the rescaling of particle masses is shown to be the key factor leading to less concentration of particles in halos than in ΛCDM, a pattern which is also observed in previous independent coupled scalar field simulations.

Key words:

1 INTRODUCTION

The nature of the dark energy (Copland *et al* 2006) driving an apparent acceleration of the universe has been a cosmological puzzle for more than a decade. Models incorporating scalar fields are the most popular proposal to explain it, those, not only because of their mathematical simplicity and phenomenological richness, but also because the scalar field is a natural ingredient of many high-energy physics theories. A scalar field contributes a single dynamical degree of freedom which can interact indirectly with other matter species through gravity or couple directly to matter, producing a fifth force on the matter which creates violations of the Weak Equivalence Principle (WEP). This second possibility of direct coupling to matter was introduced with the hope that such a coupling could potentially alleviate the coincidence problem of dark energy (Amendola 2000) and has since then attracted a great deal of attention (see, for examples, Bean & Magueijo (2001); Amendola (2004); Koivisto (2005); Lee, Liu & Ng (2006); Boehmer *et al.* (2008); Bean *et al.* (2008); Bean, Flanagan & Trodden (2008); Boehmer *et al.* (2009) and references therein). It was also investigated in the context of theoretical studies of the cosmological variation of the fine structure constant (Sandvik, Barrow & Magueijo 2002).

If there is a direct coupling between the scalar field and baryons, then the baryonic particles will experience a fifth force, which is severely constrained by observations, unless there is some special mechanism to suppress the fifth-force effects. This happens in chameleon models, where the scalar field (the 'chameleon') gains mass in high-density regions (where observations and experiments are performed) whereas the fifth force effects are confined to undetectably small distances (Khoury & Weltman 2004; Mota & Shaw 2007). A common approach which avoids such complications is to assume that the scalar field couples only to the dark matter, an idea seen frequently in models with a coupled dark sector (*e.g.* Caldera-Cabral, Maartens & Schaefer (2009); Valiviita, Maartens & Majerotto (2010); Simpson, Jackson & Peacock (2010)). In this work our scalar field will not be chameleon-like as this case has already been investigated elsewhere (Li & Zhao 2009; Zhao *et al.* 2010; Li & Zhao 2010).

A scalar field coupled to (dark) matter could affect cosmic structure formation in various ways. Firstly, the background expansion rate gets modified, which will lead to faster or slower clustering of matter particles; secondly, the coupling effectively rescales the mass of the particles for the coupled matter species, changing the source term of the Poisson equation, which receives a further contribution from den-

⋆ E-mail: b.li@damtp.cam.ac.uk
† E-mail: j.d.barrow@damtp.cam.ac.uk

sity perturbations of the scalar field; thirdly, the coupling to the scalar field produces a fifth force between matter particles, helping matter to cluster more strongly; finally, there is an extra velocity-dependent force on the coupled particles, which can be viewed either as a frictional force or as part of the fifth force under a frame transformation, and this force, being attractive, also promotes matter clustering.

Not all of these effects are always manifest. In fact, in some coupled-scalar-field models one or more then one of them could be negligible. An example is the model considered in Li & Zhao (2009, 2010), where only the third effect, *i.e.*, the fifth force, is non-negligible. This situation is also assumed in some other studies of the effect of a fifth force on structure formation, *e.g.*, the ReBEL model Nusser, Gubser & Peebles (2005), where a Yukawa-type extra force is added while the background cosmology is taken to be the same as ΛCDM.

In other, more general, models, however, a coupling between scalar field (dark energy) and (dark) matter often not only produces the fifth force, but equally likely creates other effects listed above. Examples are the models investigated in Maccio *et al.* (2004); Baldi *et al.* (2010); Li & Barrow (2010), where the modified expansion rate, varying particle mass and frictional force are all non-negligible. The situation then becomes complicated here, because these could have both positive and negative effects on the structure formation, which are difficult to disentangle.

In order to clarify the importance of all these effects, we have to make detailed analysis by suppressing one or more of these effects and then comparing the results – which is our primary aim of this work, at least for the model considered Li & Barrow (2010). In particular, we would like to see how those above effects affect the nonlinear matter power spectrum, mass function and profiles of dark matter halos. The latter is quite interesting, as it has been shown in ref. Baldi *et al.* (2010); Li & Barrow (2010) that the coupling, which is supposed to boost clustering of matter, does indeed suppress the density in the inner region of the halos, possibly due to the frictional force and/or the varying mass effects. A clarification of the importance of these effects is also relevant to the general model tests. As we mentioned above, the majority of the investigations of the fifth force to date focus only on the fifth force itself but neglect the other effects. Yet the same physics responsible for the fifth force will often create other associated effects and the latter must be taken into account for the sake of consistency. If it turns out that the fifth force effects do not dominate the others, then a model-independent test of the fifth force might be difficult to obtain in cosmology, since different models predict very different background expansion and mass variation.

Since we want to investigate the nonlinear regime, we will use the N-body simulation technique introduced in Li & Zhao (2010); Li & Barrow (2010) and also applied in Li (2010); Li, Mota & Barrow (2010a,b). Note that other approaches to N-body simulations for (coupled) scalar field and related models, without solving the scalar field equation of motion explicitly, have been also used in various previous work, *e.g.*, Maccio *et al.* (2004); Baldi *et al.* (2010); Linder & Jenkins (2003); Mainini *et al.* (2003); Kesden & Kamionkowski (2006); Springel & Farrar (2007); Farrar & Rosen (2007); Keselman, Nusser & Peebles (2009, 2010); Hellwing & Juszkiewicz (2009); Hellwing, Knollmann & Knebe (2010); Baldi (2010); Baldi & Pettorino (2010); Baldi & Viel (2010); Hellwing, Juszkiewicz & van de Weygaert (2010); De Boni *et al* (2010), while the new feature of our approach is that we solve the scalar field equation directly (in the quasi-static limit, for more details see Li & Zhao (2010); Li & Barrow (2010)).

The outline of the paper is as follows: in Sect. 2 we introduce the basic equations needed to understand the underlying physics of the model. In Sect. 3 we briefly describe the simulations we have performed for the study of the different effects of a coupled scalar field on structure formation, and then display and discuss the numerical results; we summarise and conclude in Sect. 4.

2 BASIC EQUATIONS

All the equations relevant for the simulations used here are derived and discussed in detail in Li & Barrow (2010), but to make the present work self-contained we list the minimum set necessary for us to understand the physical evolution. Instead of writing down the field equations directly, we start from a Lagrangian

$$\mathcal{L} = \frac{1}{2}\left[\frac{R}{\kappa} - \nabla^a\varphi\nabla_a\varphi\right] + V(\varphi) - C(\varphi)\mathcal{L}_{\rm DM} + \mathcal{L}_{\rm S} \qquad (1)$$

where R is the Ricci scalar, $\kappa = 8\pi G$ with G the gravitational constant, $\mathcal{L}_{\rm DM}$ and $\mathcal{L}_{\rm S}$ are respectively the Lagrangian densities for dark matter and standard model fields, φ is the scalar field, and $V(\varphi)$ its potential; the coupling function $C(\varphi)$ characterises the coupling between φ and dark matter. Given $V(\varphi)$ and $C(\varphi)$ a model is then fully specified.

Varying the total action with respect to the metric g_{ab}, we obtain the following expression for the total energy-momentum tensor in this model:

$$\begin{aligned} T_{ab} &= \nabla_a\varphi\nabla_b\varphi - g_{ab}\left[\frac{1}{2}\nabla^c\nabla_c\varphi - V(\varphi)\right] \\ &\quad + C(\varphi)T^{\rm DM}_{ab} + T^{\rm S}_{ab} \end{aligned} \qquad (2)$$

where $T^{\rm DM}_{ab}$ and $T^{\rm S}_{ab}$ are the energy-momentum tensors for (uncoupled) dark matter and standard model fields. The existence of the scalar field and its coupling change the form of the energy-momentum tensor, and so modify the cosmology from background expansion to structure formation.

The coupling to scalar field produces a direct interaction (a.k.a. the fifth force) between dark matter particles, due to the exchange of scalar quanta. This is best illustrated by the geodesic equation for dark matter particles

$$\frac{d^2\mathbf{r}}{dt^2} = -\vec{\nabla}\Phi - \frac{C_\varphi(\varphi)}{C(\varphi)}\vec{\nabla}\varphi \qquad (3)$$

where $\mathbf{r}$ is the position vector, t the (physical) time, Φ the Newtonian potential and $\vec{\nabla}$ is the spatial derivative. $C_\varphi = dC/d\varphi$. The second term on the right-hand side is the fifth force and only exists for coupled matter species (dark matter in our model). The fifth force also changes the clustering properties of the dark matter. Note that on very large scales φ is homogeneous and the fifth force vanishes.

In order to solve the two equations above numerically we need to solve both the time evolution and the spatial

distribution of φ, and this could be done using the scalar field equation of motion

$$\nabla^a\nabla_a\varphi + \frac{dV(\varphi)}{d\varphi} + \rho_{\rm DM}\frac{dC(\varphi)}{d\varphi} = 0 \tag{4}$$

or equivalently

$$\nabla^a\nabla_a\varphi + \frac{dV_{eff}(\varphi)}{d\varphi} = 0 \tag{5}$$

where we have defined

$$V_{eff}(\varphi) = V(\varphi) + \rho_{\rm DM}C(\varphi). \tag{6}$$

The background evolution of φ can be solved easily once we know the current $\rho_{\rm DM}$, because $\rho_{\rm DM} \propto a^{-3}$. We can then divide φ into two parts, $\varphi = \bar{\varphi} + \delta\varphi$, where $\bar{\varphi}$ is the background value, and $\delta\varphi$ the (not necessarily small and linear) perturbation, and subtract the background scalar-field equation of motion from the full equation to obtain the equation of motion for $\delta\varphi$. In the quasi-static limit where we can neglect time derivatives of $\delta\varphi$ compared with its spatial derivatives (which turns out to be a good approximation for our simulations, because the simulation box is much smaller than the observable Universe), we get

$$\vec{\nabla}^2\varphi = \frac{dC(\varphi)}{d\varphi}\rho_{\rm DM} - \frac{dC(\bar{\varphi})}{d\bar{\varphi}}\bar{\rho}_{\rm DM} + \frac{dV(\varphi)}{d\varphi} - \frac{dV(\bar{\varphi})}{d\bar{\varphi}} \tag{7}$$

where $\bar{\rho}_{\rm DM}$ is the background dark-matter density.

Once $\rho_{\rm DM}$ is known on a grid, we can then solve $\delta\varphi$ on that grid using a nonlinear Gauss-Seidel relaxation method (in our simulations we have modified `MLAPM` Knebe, Green & Binney (2001), a publicly available N-body code using a self-adaptive refined grid so that high resolutions can be achieved in high-density regions). Since $\bar{\varphi}$ is also known, we can then obtain the full solution of $\varphi = \bar{\varphi} + \delta\varphi$. This completes the computation of the source term for the Poisson equation:

$$\vec{\nabla}^2\Phi = \frac{\kappa}{2}\left[C(\varphi)\rho_{\rm DM} - C(\bar{\varphi})\bar{\rho}_{\rm DM} + \delta\rho_{\rm B} - 2\delta V(\varphi)\right], \tag{8}$$

where $\delta\rho_{\rm B} \equiv \rho_{\rm B} - \bar{\rho}_{\rm B}$ and $\delta V(\varphi) \equiv V(\varphi) - V(\bar{\varphi})$ are respectively the density perturbations of baryons and scalar field (note that we have neglected perturbations in the kinetic energy of the scalar field because they are always very small for our model).

We can then solve Eq. (8) using a linear Gauss-Seidel relaxation method on the same grid to obtain Φ. With both Φ and φ in hand, Eq. (3) can then be used to compute the forces on the dark matter particles, and once we have the forces, we can perform all the standard N-body operations such as momentum-kick, position-drift, time-stepping and so on.

Eqs. (2 - 8) are all what we need to complete an N-body simulation for coupled scalar field cosmology Li & Barrow (2010), and from them we can see where the effects of the scalar-coupling enter:

(i) The modified background expansion rate mainly affect the particle movements and time-stepping, *i.e.*, Eq. (3), because in the simulations we use the cosmic scale factor a, instead of t, as the time variable and $d/dt = \dot{a}d/da$.

(ii) The varying mass effect is seen directly from Eq. (8), which shows that the contribution of $\rho_{\rm DM}$ to the source term of the Poisson equation is normalised by $C(\varphi)$ which is different from 1 in general. In our model it is not true that the mass of dark matter particles is really varying, but the net effect is just equivalent to such a variation.

(iii) The fifth force appears explicitly on the right-hand side of Eq. (3), but is only for coupled matter species (dark matter).

(iv) The velocity-dependent (or frictional) force hides in the fact that Eqs. (3, 7) are given in *different* gauges: Eq. (3) is the force for a dark-matter particle and is given in that particle's rest frame, while Eq. (7) is written in the fundamental observer's frame. As a result, in order to use the $\delta\varphi$ solved from Eq. (7) in Eq. (3), we need to perform a frame transform $\vec{\nabla}\delta\varphi \to \vec{\nabla}\delta\varphi + a\dot{\bar{\varphi}}\dot{\mathbf{x}}$, where $\dot{\mathbf{x}}$ is the comoving velocity of the particle relative to the fundamental observer. This force is therefore expressed as $-\frac{C_{,\varphi}}{C}a\dot{\varphi}\dot{\mathbf{x}}$, and obviously the faster a particle travels the stronger such force it feels.

3 SIMULATIONS AND RESULTS

3.1 Model and Simulation Details

As is mentioned above, a coupled scalar field model is fully specified given the exact forms of the bare potential $V(\varphi)$ and coupling function $C(\varphi)$. Here we shall choose the same model as Li & Barrow (2010), with an inverse power-law potential

$$V(\varphi) = \frac{\Lambda^4}{(\sqrt{\kappa}\varphi)^\alpha} \tag{9}$$

and the exponential coupling

$$C(\varphi) = \exp\left(\gamma\sqrt{\kappa}\varphi\right), \tag{10}$$

where Λ is a constant with mass dimension and Λ^4 is of order the dark-energy density today; α, γ are dimensionless parameters. We choose $\alpha = 0.1$ so that the potential is flat enough to enable a slow-roll of φ (which accounts for the dark energy); for γ, we choose $|\gamma| \sim \mathcal{O}(0.1)$ and $\gamma < 0$ so that both $V(\varphi)$ and $V_{eff}(\varphi)$ are of runaway type[1].

Li & Barrow (2010) have given a very detailed description of the technicalities of the N-body simulations for coupled scalar-field theories, and so we shall not repeat this methodology here. Roughly speaking, the most important distinction between our simulation and others is that we have solved the scalar field equation of motion explicitly on a grid (in the quasi-static limit). Because of this, we have been able to solve the fifth force (and the frictional force) numerically without recourse to analytical approximations. Furthermore, we have incorporated both *time* and the *space* variations of the particle mass (or more rigorously of $C(\varphi)$) because we have spatial information about the scalar field distribution.

Since our aim is to test the significance of each of the four above-named effects, we choose to suppress one of them at one time. Together with the full model, where all effects are included, and the ΛCDM model for comparison, we then have six models to simulate. Furthermore, we consider two

[1] Since $V_{eff}(\varphi)$ is of runway type there is nothing to stop the scalar field rolling down V_{eff}, so typically we shall have $\sqrt{\kappa}\varphi \sim \mathcal{O}(1)$ today, which makes $C(\varphi)$ deviate significantly from 1. Increasing $|\gamma|$ will makes this problem more severe, and this is why we set $|\gamma| \sim \mathcal{O}(0.1)$ rather than $\mathcal{O}(1)$.

simulation no.	α	γ	simulation description
L	0.0	0.00	pure ΛCDM
S1	0.1	−0.10	full coupled scalar field
S1a	0.1	−0.10	scalar field with the frictional force $-\frac{C_\varphi}{C}a\dot{\bar{\varphi}}\dot{\mathbf{x}}$ suppressed
S1b	0.1	−0.10	scalar field with the fifth force $-\frac{C_\varphi}{C}\vec{\nabla}\delta\varphi$ suppressed
S1c	0.1	−0.10	scalar field with the (time *and* spatial) variation of mass $C(\varphi)$ removed
S1d	0.1	−0.10	scalar field with a ΛCDM background expansion
S2	0.1	−0.20	full coupled scalar field
S2a	0.1	−0.20	scalar field with the frictional force $-\frac{C_\varphi}{C}a\dot{\bar{\varphi}}\dot{\mathbf{x}}$ suppressed
S2b	0.1	−0.20	scalar field with the fifth force $-\frac{C_\varphi}{C}\vec{\nabla}\delta\varphi$ suppressed
S2c	0.1	−0.20	scalar field with the (time *and* spatial) variation of mass $C(\varphi)$ removed
S2d	0.1	−0.20	scalar field with a ΛCDM background expansion

different choices of the coupling strength γ. So in total we have 11 models, details of which are summarised in the following table:

The physical parameters we adopt in all simulations are as follows: the present-day dark-energy fractional energy density $\Omega_{\rm DE} = 0.743$ and $\Omega_m = \Omega_{\rm CDM} + \Omega_{\rm B} = 0.257$, $H_0 = 71.9$ km/s/Mpc, $n_s = 0.963$, $\sigma_8 = 0.761$. The size of simulation box is $64h^{-1}$ Mpc with $h = H_0/(100$ km/s/Mpc). In all these simulations, the mass resolution is $1.114\times10^9h^{-1}\,M_\odot$, the particle (both dark matter and baryons) number is 256^3, the domain grid is a $128\times128\times128$ cubic and the finest refined grids have 16384 cells on each side, corresponding to a force resolution of order $12h^{-1}$ kpc.

3.2 Numerical Results

For the numerical results, we display the matter power spectrum, mass function and halo density profiles for the 11 runs described above, and discuss how they are affected by the individual effects from the scalar coupling.

Before going to the details, it is helpful to have a quick browse about the scalar-coupling effects: (I) The velocity-dependent force $-\frac{C_\varphi}{C}a\dot{\bar{\varphi}}\dot{\mathbf{x}}$ is parallel to the direction of motion ($\dot{\mathbf{x}}$); because $\dot{\bar{\varphi}} > 0$ and $\gamma < 0$, so it accelerates the particles. (II) The fifth force $-\frac{C_\varphi}{C}\vec{\nabla}\delta\varphi$ in this model is found (Li & Barrow 2010) to be parallel to gravity and the ratio between the magnitudes of the two is $2\gamma^2$ to a high precision; as such the fifth force both accelerates the particles and increases their mutual attraction. (III) $C(\varphi) < 1$ because $\gamma < 0$ and $\varphi > 0$, so that the contribution of dark matter density to the source of Poisson equation gets weakened, effectively reducing the gravity force and causing less mutual attraction between particles and less clustering. (IV) For the chosen model and physical parameters, the background expansion rate decreases as $|\gamma|$ increases (Li & Barrow 2010), making matter particles less diluted and cluster more. These facts are important to bear in mind for discussions below.

3.2.1 Matter Power Spectrum

In Fig. 1 we have plotted the fractional change of the nonlinear matter power spectrum with respect to ΛCDM prediction for the simulations S1 and S1a-d. Roughly, the deviation from the black solid curve (S1) indicates the importance of a given coupled-scalar effect: the larger the deviation is, the more that specific effect contributes to the full coupled scalar field result. Of least importance is the velocity-dependent force $-\frac{C_\varphi}{C}a\dot{\bar{\varphi}}\dot{\mathbf{x}}$ (green dotted curves). As this force accelerates particles, it makes particles collapse faster to the regions of high density, and thus slightly enhances the clustering. Consequently, suppressing it will decrease $P(k)$. Of the second least importance is the fifth force term $-\frac{C_\varphi}{C}\vec{\nabla}\delta\varphi$ (blue dashed curves). It not only accelerates particles (towards the high-density regions) but also increases the central force. As such its effect is also to enhance the clustering of matter and neglecting it leads to smaller $P(k)$ on all scales.

Next is the varying mass effect (purple dash-dot curves), the presence of which reduces the source of the Poisson equation and thus weakens gravity. Obviously its effect is to produce weaker clustering of matter particles and dropping it will increase $P(k)$ significantly.

he most important coupled-scalar effect comes from the modified background expansion rate (pink dash-dot-dot-dot curves). As mentioned above, if the universe expands more slowly (as in the case of our coupled scalar field model Li & Barrow (2010)), then particles are less diluted and have more time to cluster, resulting in a larger $P(k)$. Changing the background expansion to ΛCDM (*i.e.*, increasing it) simply produces a smaller $P(k)$ than the full simulation. Note that the pink curves are consistently below zero, indicating that although simulation S1d uses the same background expansion rate as simulation L, $P(k)$ is smaller than for the latter, a result that is again due to the fact that in S1d the varying mass effect is taken into account, weakening the matter clustering and decreasing $P(k)$ (as discussed above, the fifth force does have the opposite effect but cannot overcome this).

In Fig. 2 we have shown the same plots, but for the models S2 and S2a-d. All the above analysis still applies but the effects just become stronger. Interestingly, the most important coupled-scalar effects (at least for our models, which are typical ones) are not those of the fifth force, but are instead the modified background expansion rate and varying mass of matter particles. This is understandable, because the magnitude of the fifth force is about $2\gamma^2$ times that of gravity, and for our S1 and S2 simulations the values are 0.02 and 0.08 respectively, while at the same time the deviations of $C(\varphi)$ from 1 for these two models are ~ 0.1 and ~ 0.3 Li & Barrow (2010) and so are far stronger.

This means that one must be cautious about adding a Yukawa-type fifth force to the N-body simulation, while keeping all other things the same as in ΛCDM, because the

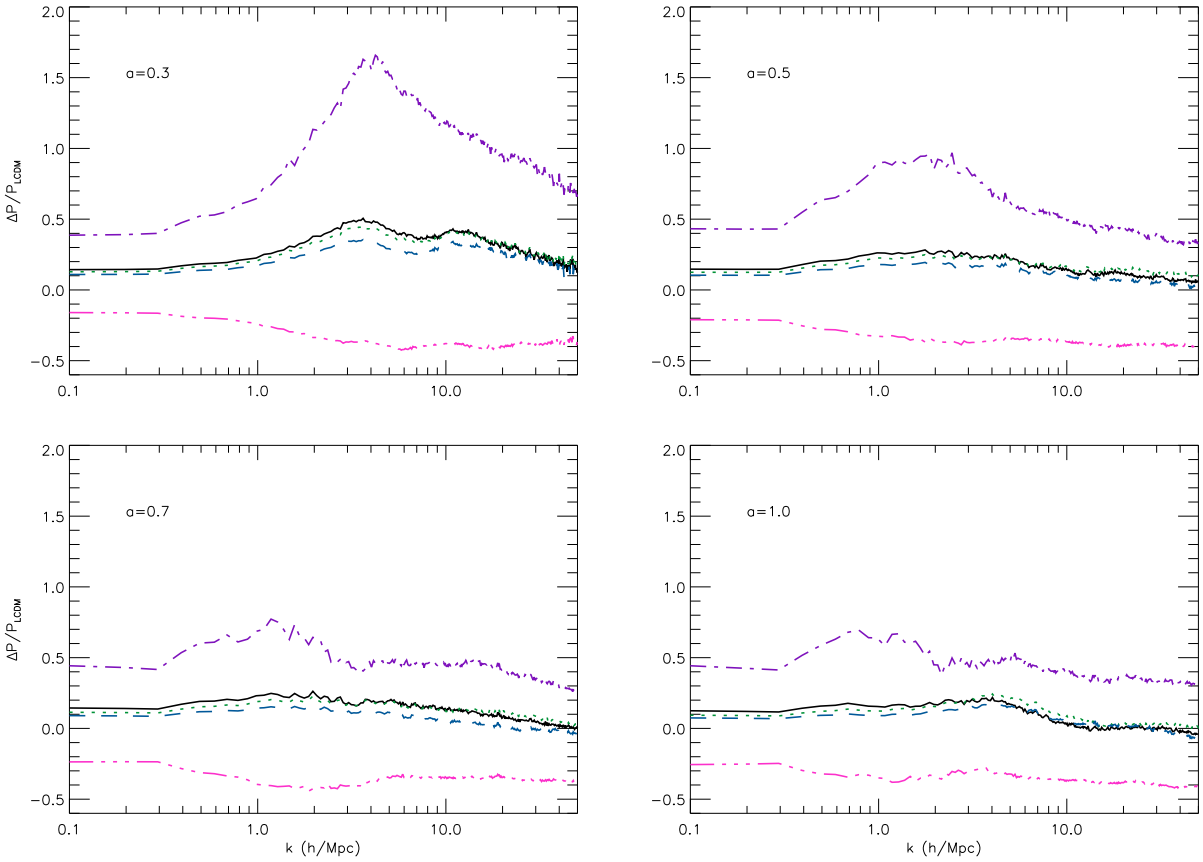

Figure 1. (Colour Online) Fractional changes of the nonlinear matter power spectrum with respect to the ΛCDM result at four different output times: $a = 0.3$ (*upper left panel*), $a = 0.5$ (*upper right panel*), $a = 0.7$ (*lower left panel*) and $a = 1.0$ (*lower right panel*). In each panel the results of the simulations S1 (full coupled scalar simulation), S1a (frictional force suppressed), S1b (fifth force suppressed), S1c (mass variation removed) and S1d (ΛCDM background) are represented by the black solid, green dotted, blue dashed, purple dash-dot and pink dash-dot-dot-dot curves respectively.

fifth force often introduces associated effects which are more important

3.2.2 Mass Functions

Fig. 3 shows the mass functions of the simulations S1 and S1 compared with that of ΛCDM (L). Again, the deviation from the full simulation result (black solid curve) indicates the order of importance of the individual effects. The two least important factors are once more the velocity-dependent force $-\frac{C_\varphi}{C}a\dot{\varphi}\dot{\mathbf{x}}$ and the fifth force $-\frac{C_\varphi}{C}\vec{\nabla}\delta\varphi$, both of which, according to our above analysis, enhance matter cluster: suppressing them causes less clustering of matter and smaller mass functions. Their influences however are quite weak, in particular that of the velocity-dependent force.

The second important effect is the variation of mass or $C(\varphi)$. In case $C(\varphi) < 1$ then, as mentioned above, the mutual gravitational interaction between particles becomes weaker and particles will cluster less strongly. As a result, removing this effect enhances the matter clustering and leads to massive halos being created in larger abundance.

The most influential effect from a coupled scalar field is the modified background expansion. Changing it to a ΛCDM background (which is faster) significantly underestimates the mass function, because particles get more diluted and have less time to clump.

The corresponding results for models S2 and S2a-d are summarized in Fig. 4, and they show the same qualitative trend as Fig. 3 but the effects are just stronger, due to the stronger coupling $|\gamma|$ and thus more dramatic evolution of the scalar field φ (which means that $C(\varphi)$ deviate more from unity and the expansion rate is decreased more compared to simulation L).

Although the mass function does show the imprint from a fifth force, this is by no means unique and could easily be dominated over by the associated coupled scalar effects like modified background expansion rate or varying particle mass.

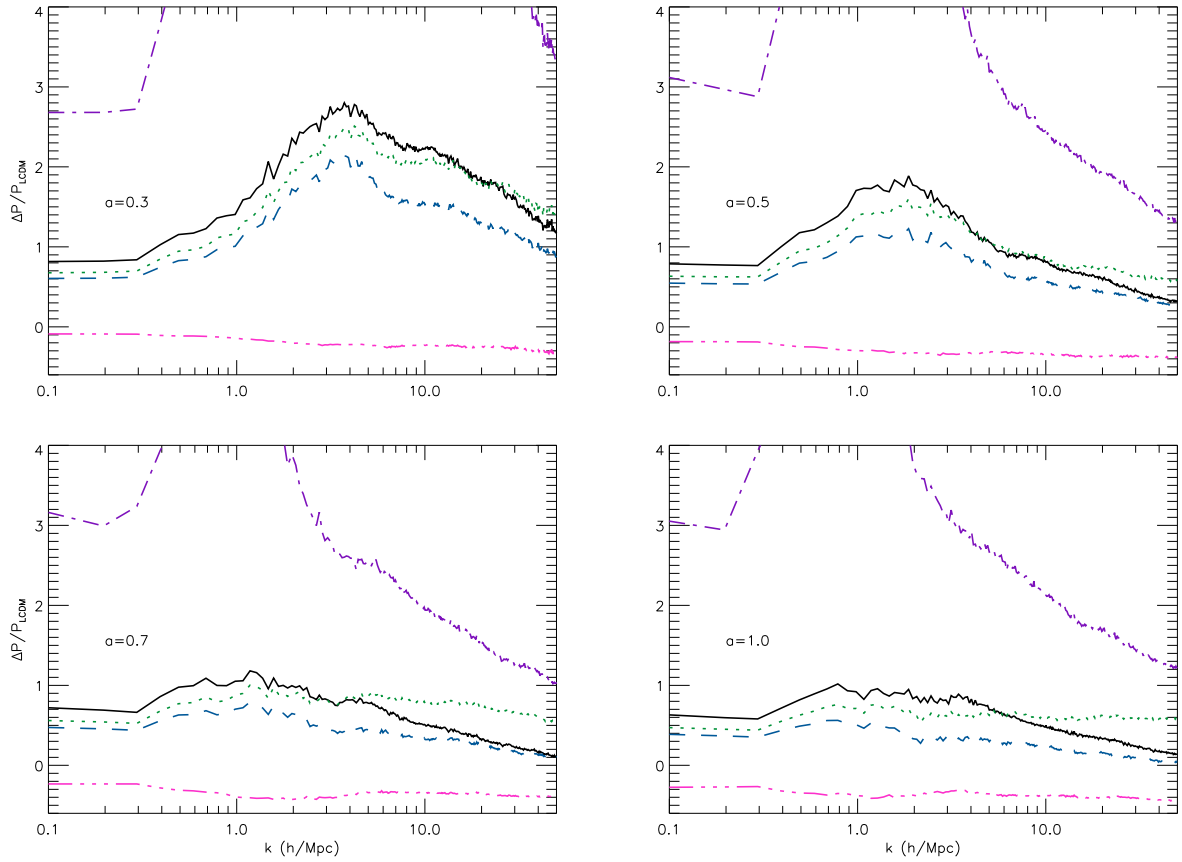

Figure 2. (Colour Online) The same as Fig. 1, but for the models where $\gamma = -0.20$, *i.e.*, S2 and S2a-d.

3.2.3 Halo Density Profiles

Internal density profiles of the dark matter halos are another area where the scalar field coupling could leave interesting imprints. For example, Li & Zhao (2010) showed that for a chameleon-like scalar field model the density profiles could be either increased or decreased significantly by the scalar coupling, depending on the environment of the halos. For the models considered here, Baldi *et al.* (2010); Li & Barrow (2010) have given convincing evidence that the internal density profile has similar shape to ΛCDM, but could be somewhat suppressed in the very inner parts.

As an explicit example, Fig. 5 shows the density profiles of the most massive halo from each box for simulations L, S1 and S1a-d. The suppression of the full simulation result (black solid curve) compared with the ΛCDM prediction (thick solid dashed curve) is evident below $R \sim 400h^{-1}$Kpc.

If the velocity-dependent force $-\frac{C_\varphi}{C}a\dot{\bar{\varphi}}\dot{\mathbf{x}}$ is given up (green dotted curve), then the suppression is moderated. As discussed in Baldi *et al.* (2010), this is because this force effectively accelerates particles, making them travel faster and so increases the total kinetic energy of the particles inside the halo. As a result, removing this force will leave the particles with less kinetic energy, meaning that they more easily fall towards the halo centre. Unlike in Baldi *et al.* (2010), here this effect is not the major one (see below).

The fifth force $-\frac{C_\varphi}{C}\vec{\nabla}\delta\varphi$ is slightly more complicated. On one hand, it speeds the particles up, increasing their kinetic energy; on the other, it enhances the mutual attraction between particles, increasing the (magnitude of the) potential energy of the halo. These two effects are just opposite, as deepening the potential of a halo will pull more particles towards the centre and thus increase the concentration. For simulation S1, it seems that the former effect takes over, and dropping the fifth force (blue dashed curve) simply decreases the kinetic energy of particles and make them more concentrated towards the halo centre.

The effect of the varying-mass factor $C(\varphi) < 1$ is unambiguously to suppress the over-density inside the halos, as it decreases the source of the Poisson equation and so weakens gravity, making the potential shallower. Dropping it simply deepens the potential and attracts more particles to the inner region of the halo (purple dash-dotted curve).

Finally, changing (increasing) the background expansion rate relative to ΛCDM again leads to less clustering of particles, and thus lower density profiles in the halos (pink dash-dot-dot-dot curves).

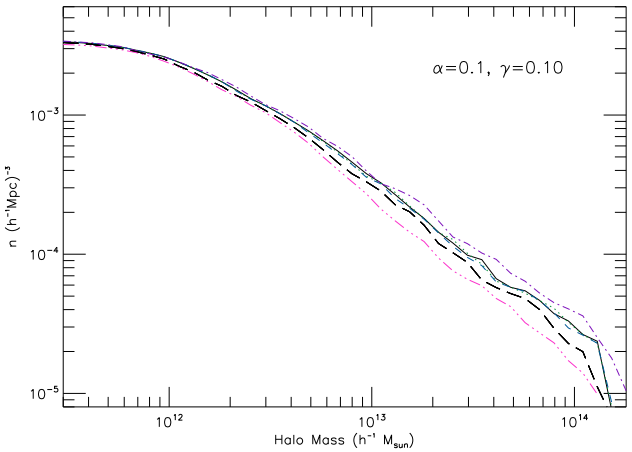

Figure 3. (Colour Online) The mass functions for the models S1 (black solid curve), S1a (green dotted), S1b (blue dashed), S1c (purple dash-dot) and S1d (pink dash-dot-dot-dot) compared to the ΛCDM result (thick long dashed curve). The horizontal axis is the virial mass of halos, in unit of $h^{-1}M_{\odot}$; the vertical axis is the halo number density in the simulation box, in units of $\left(h^{-1}\mathrm{Mpc}\right)^{-3}$.

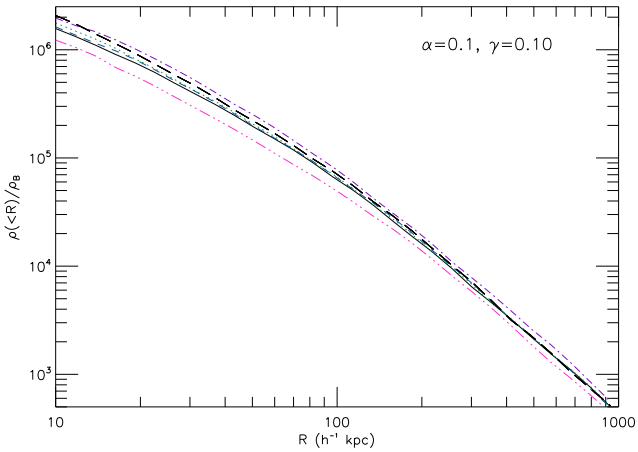

Figure 5. (Colour Online) The internal density profile of the most massive halo in the simulation box for the models S1 (black solid curve), S1a (green dotted), S1b (blue dashed), S1c (purple dash-dot) and S1d (pink dash-dot-dot-dot) compared to the ΛCDM result (thick long dashed curve). The horizontal axis is the radius from halo centre, in unit of h^{-1}Kpc, and the vertical axis is the overdensity.

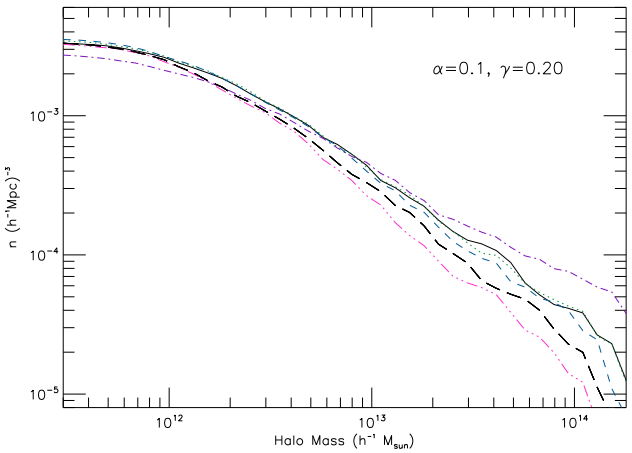

Figure 4. (Colour Online) The same as Fig. 3, but for models S2 and S2a-d.

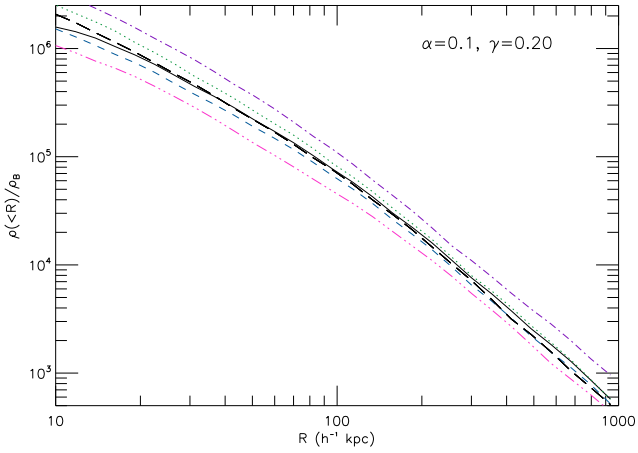

Figure 6. (Colour Online) The same as Fig. 5, but for models S2 and S2a-d.

It is worth noting that although the velocity-dependent force, fifth force, and varying mass all contribute to suppressing the internal density of the halo, the varying mass contributes most, while the fifth force contributes least. This differs from the finding of Baldi *et al.* (2010), that the velocity-dependence force is the determining factor, possibly due to differences in the models and their treatments. The fact that the velocity-dependent force dominates over the fifth force (which is different from what we have seen for matter power spectrum and mass function) is not surprising, for, as mentioned above, the fifth force is set to increase both the kinetic and potential energies, two effects somehow cancelling each other out.

Fig. 6 displays the same results for the models S2 and S2a-d, and we can see qualitatively similar but stronger trends. The notable thing is that in this case suppressing the fifth force further lowers the inner density of the halo, an indication that here the deepening of potential dominates over the increase in kinetic energy (both are due to the fifth force).

Above we have just discussed the results for one specific halo (the most massive one), while what we are more interested in is the general behaviour. For this we have selected 10 out of the most massive halos and computed their average density profile. The results for simulations S1 and S1a-d are shown in Fig. 7, in which we have plotted the fractional change of the averaged halo internal density with respect to the ΛCDM result. From this figure we see again that overall the internal density in the inner region of halos is lower in (full) coupled scalar field models than in ΛCDM. Both the velocity-dependent force and varying mass tend to decrease the inner density, and both the fifth force and the modified

[tbp]

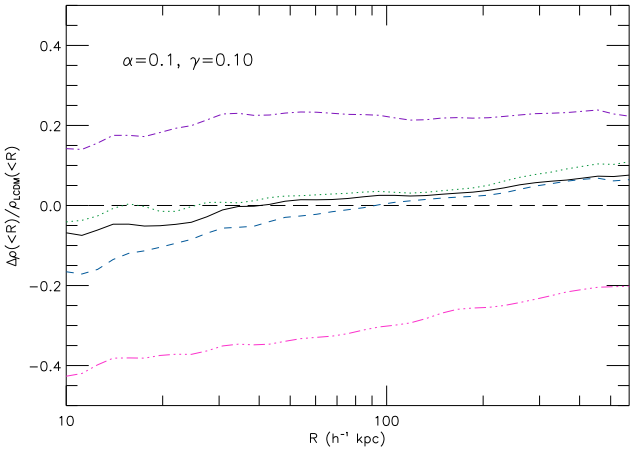

Figure 7. (Colour Online) The fractional change of averaged halo density profile for the models S1 (black solid curve), S1a (green dotted), S1b (blue dashed), S1c (purple dash-dot) and S1d (pink dash-dot-dot-dot) compared to the ΛCDM result (thick long dashed curve). The horizontal axis is the distance from halo centre, in unit of h^{-1}Kpc, and the vertical axis is the fractional change of density with respect to the ΛCDM prediction.

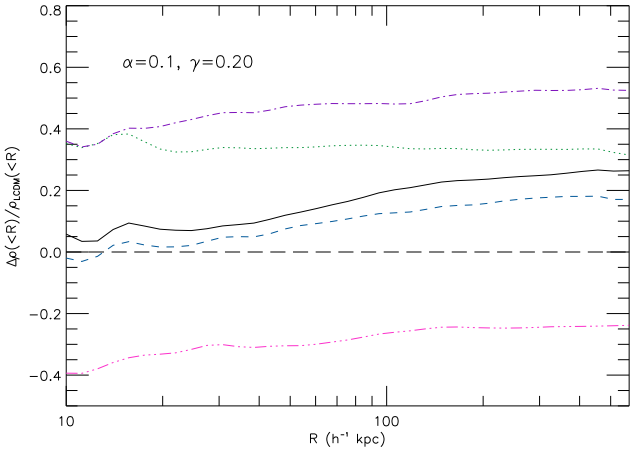

Figure 8. (Colour Online) The same as Fig. 7, but for models S2 and S2a-d.

(slower) background expansion help increase it. The effects from the varying mass and modified background expansion are dominant while the other two effects are minor, confirming our observed pattern from a single halo (Fig. 5).

We see a similar result for the models S2 and S2a-d, as shown in Fig. 8. A notable difference here, however, is that the velocity-dependent force becomes more important than in S1. Indeed, it is as dominant as the varying mass effect in the inner region of the halos, though it is still subdominant in the outer region; this at least shows some agreement with Baldi *et al.* (2010). Note again that the fifth force is the least important amongst all the four effects, which means that using a simulation with ΛCDM plus a Yukawa-type fifth force we would be unable to catch the (probably) most significant effects from a coupled scalar field.

4 SUMMARY AND CONCLUSION

To summarise: in this paper, with the aid of N-body simulations, we have investigated the different impacts of a coupled scalar field on cosmic structure formation, and assessed their qualitative effects and quantitative importance. The scalar field coupling influences the structure formation mainly through a velocity-dependent force, a fifth force, a modification of the particle mass (or the source of the Poisson equation) and a modified background expansion rate. We have investigated how dropping each one of these factors leaves imprints on the key structure formation observables, like matter power spectrum, mass function and the internal density profile of dark matter halos.

For the matter power spectrum and mass function, we find that the modified background expansion rate is by far the most important effect that the scalar-coupling can have, followed in turn by the variation of particle mass, fifth force and the velocity-dependent force. The cosmic expansion becomes slower than that in ΛCDM due to the scalar field, which means that structure has more time to form. The fifth force increases the mutual attractive force between particles, strengthening the collapse of overdense regions; both the fifth force and the velocity-dependent force could speed up particles, making the collapse faster. As a result, all these three effects help boost the growth of structure. On the other hand, the source of the Poisson equation is decreased due to the coupling function $C(\varphi)$, resulting in weaker gravity and weakened structure formation.

The internal density profiles for dark matter halos are more interesting, and as we have seen the combined effect of a scalar-coupling can be to suppress the density of the inner regions of the halos (or to distribute particles more towards outer regions). As one might expect, the modified cosmic expansion rate is again the most important scalar-coupling effect here, and with it dropped there will be less structure formation and lower halo density profiles. The variation of particle masses, or the modification to the source of the Poisson equation, is the second largest single effect, followed by the velocity-dependent force and fifth force. Roughly speaking, the particles tend to move towards (by a process of relaxation and virialisation) the inner regions of halos if their kinetic energy is reduced and/or the central potential gets deeper, and vice versa (Baldi *et al.* 2010). In this regard, the velocity-dependent force speeds up particles and the variation of particle mass weakens the central potential, both in favour of lower central densities in halos (cf. Figs. 5 - 8). The fifth force has two opposite effects – to speed up particles (and so increase the kinetic energy) and to deepen the total potential. They cancel each other out to a certain extent, so making the fifth force less influential in determining the density profiles (than the velocity-dependent force)

Our result is marginally consistent with previous analyses (*e.g.*, Baldi *et al.* (2010)) of the halo density profiles, but shows discrepancy about whether the velocity-dependent force is more important than the varying particle mass or not. The difference might be due to different model specifications and treatments.

One of our most important results is that in many cases the fifth force, which is the most well-known consequence of a coupling between matter and a scalar field, is not the most important in affecting the structure formation. The

key point is that, when we introduce such a coupling, other new effects are also brought in, and these can often be much more influential. It is in this regard that the advantages of full N-body simulations Maccio *et al.* (2004); Baldi *et al.* (2010); Li & Zhao (2009, 2010); Li & Barrow (2010), which take full account of all associated effects, are increasingly significant.

ACKNOWLEDGMENTS

The work described in this paper has been performed on COSMOS, the UK National Cosmology Supercomputer. The matter power spectrum and halo properties are computed using POWMES (Colombi *et al* 2009) and MHF Gill, Knebe & Gibson (2004) respectively. We thank Marco Baldi for comments on the draft. B. Li is supported by a Junior Research Fellowship at Queens' College, Cambridge, and the Science and Technology Facility Council of the United Kingdom.

REFERENCES

Amendola L., 2000, PRD62, 043511
Amendola L., 2004, PRD69, 103524
Baldi M., 2010, arXiv:1005.2188 [astro-ph.CO]
Baldi M., Pettorino V., 2010, arXiv: 1006.3761 [astro-ph.CO]
Baldi M., Viel M., 2010, arXiv: 1007.3736 [astro-ph.CO]
Baldi M., Pettorino V., Robbers G., Springel V., 2010, MNRAS, 403, 1684
Bean R., Magueijo J., 2001, Phys. Lett. B17, 177
Bean R., Flanagan E. E., Laszlo I., Trodden M., 2008, PRD78, 123514
Bean R., Flanagan E. E., Trodden M., 2008, PRD78, 023009
Boehmer C. G., Caldera-Cabral G., Lazkoz R., Maartens R., 2008, PRD78, 023505
Boehmer C. G., Caldera-Cabral G., Chan N., Lazkoz R., Maartens R., 2008, PRD81, 083003
Caldera-Cabral G., Maartens R., Schaefer B. M., 2009, JCAP, 0907, 027
Colombi S., Jaffe A., Novikov D., Pichon C., 2009, MNRAS, 393, 511
Copeland E., Sami M., Tsujikawa S., 2006, Int. J. Mod. Phys. D, 15, 1753
De Boni C., Dolag K., Ettori S., Moscardini L., Pettpromp V., Baccigalupi C., 2010, arXiv: 1008.5376 [astro-ph.CO]
Farrar G. R., Rosen R. A., 2007, PRL, 98, 171302
Gill S. P. D., Knebe A., Gibson B. K., 2004, MNRAS, 351, 399
Hellwing W. A., Juszkiewicz R., 2009, PRD80, 083522
Hellwing W. A., Juszkiewicz R., van de Weygaet R., 2010, arXiv: 1008.3930 [astro-ph]
Hellwing W. A., Knollmann S. R., Knebe A., 2010, MNRAS, 408, L104
Kesden M., Kamionkowski M., 2006, PRL, 97, 131303; PRD74, 083007
Keselman J. A., Nusser A., Peebles P. J. E., 2009, PRD80, 063517
Keselman J. A., Nusser A., Peebles P. J. E., 2009, PRD81, 063521
Khoury J., Weltman A., 2004, PRD69, 044026
Knebe A., Green A., Binney J., 2001, MNRAS, 325, 845
Koivisto T, 2005, PRD72, 043516
Lee S., Liu G. -C., Ng K. -W., 2006, PRD73, 083516
Li B., 2010, arXiv:1009.1406 [astro-ph.CO]
Li B., Barrow J. D., 2010, arXiv:1005.4231 [astro-ph.CO]
Li B., Zhao H., 2009, PRD80, 044027
Li B., Mota D. F., Barrow J. D., 2010, arXiv:1009.1396 [astro-ph.CO]
Li B., Mota D. F., Barrow J. D., 2010, arXiv:1009.1400 [astro-ph.CO]
Li B., Zhao H., 2010, PRD81, 104047
Linder E. V., Jenkins A., 2003, MNRAS, 346, 573
Mainini R., Maccio A. V., Bonometto S. A., Klypin A., 2003, ApJ, 599, 24
Maccio A. V., Quercellini C., Mainini R., Amendola L., Bonometto S. A., 2004, PRD69, 123516
Mota D. F., Shaw D. J., 2007, PRD75, 063501
Nusser A., Gubser S. S., Peebles P. J. E., 2005, PRD71, 083505
Sandvik H., Barrow J. D., Magueijo J., 2002, PRL88, 031302
Simpson, F., Jackson B. M., Peacock J. A., 2010, arXiv:1004.1920 [astro-ph.CO]
Springel V., Farrar G. R., 2007, MNRAS, 380, 911
Valiviita J., Maartens R., Majerotto E., 2010, MNRAS, 402, 2355
Zhao H., Maccio A. V., Li B., Hoekstra H., Feix M., 2010, ApJ, L712, 179